REFRACTION OF OBLIQUE SHOCK WAVE FRONT AT BOUNDARY WITH LESS RIGID MEDIUM

A. N. Dremin and G. I. Kanel'

Approximate methods are presented for calculating the unloading polars (we replace the isentrope by a broken line on each segment of which the sound speed is constant) and speed of sound behind the shock wave front in dense condensed media. The refraction parameters found with the aid of these calculations are well confirmed experimentally. Equations are given for calculating the magnitude of the critical angle of regular reflection of an oblique shock wave at the boundary with a less rigid medium and the magnitude of the angle corresponding to the maximal flow deflection on the shock polar.

The reflection and refraction of an oblique shock wave at the interface with a material having greater dynamic stiffness were examined in [1-3]. In this case the reflected wave is a shock wave. The parameters of the reflected and refracted shock waves are determined graphically in the coordinates: p = pressure, θ = angle of deflection of the flow at the intersection of the shock polar of the second medium with the shock polar for the reflected shock wave in the first medium. However, if the second medium has less dynamic stiffness the reflected wave is a fan-shaped rarefaction wave (Fig. 1). Then the refraction parameters are defined by the intersection of the shock polar of the second medium with the unloading polar of the first medium [4]. The unloading polars are constructed by calculating the flow in the Prandtl-Meyer rarefaction wave [4, 5]. However the exact calculation for materials with arbitrary equation of state is quite complex. In the present paper we propose an approximate method for calculating Prandtl-Meyer flow for condensed media which gives good agreement with experimental data. The solution of the problem of oblique shock wave front refraction when transitioning into a medium with lower dynamic stiffness is necessary, for example, in calculating the shock compression parameters under explosive welding conditions and under the conditions of shock compression of specimens in preservation ampules.

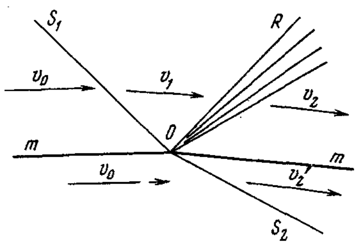

Fig 1. Refraction of oblique shock wave front at boundary with less rigid medium: S_1 = incident shock wave front; S_2 = refracted shock wave front; R = Prandtl-Meyer rarefaction wave; mom = interface. Arrows show direction of flow in coordinate system fixed with point O.

1. Approximate Calculation of Flow in Prandtl-Meyer Rarefaction Wave. Prandtl-Meyer flow is isentropic and is described in cylindrical coordinates by the following system of momentum and mass conservation equations

$$v_\varphi = \frac{dv_r}{d\varphi}, \qquad v_\varphi\left(\frac{dv_\varphi}{d\varphi} + v_r\right) = -\frac{1}{\rho}\frac{dp}{d\varphi}$$
$$\rho v_r + \frac{d}{d\varphi}(\rho v_\varphi) = 0 \tag{1.1}$$

Here v_φ and v_r are respectively the angular and radial components of the flow velocity v, φ is the coordinate angle, ρ density, p pressure. The equations (1.1) are written under the assumption that all the parameters are constant along the coordinate radius. The last two equations imply equality of the flow velocity-angular component to the local speed of sound

$$v_\varphi = c = (\partial p / \partial \rho)_S^{1/2}$$

For the approximate calculation we propose to replace the isentrope by a broken line on each segment of which the speed of sound is constant (Fig. 2). For c = v_φ = const the Eq. (1.1) takes the form

Moscow. Translated from Zhurnal Prikladnoi Mekhaniki i Tekhnicheskoi Fiziki, Vol. 11, No. 3, pp. 140-144, May-June, 1970. Original article submitted October 20, 1969.

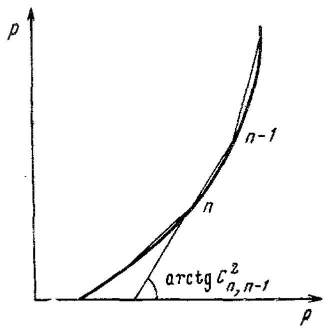

Fig. 2

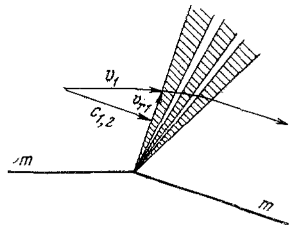

Fig. 3

Fig. 2. Construction of approximate isentrope.

Fig. 3. Prandtl-Meyer rarefaction wave when isentrope is broken curve. Rarefaction takes place in shaded zones.

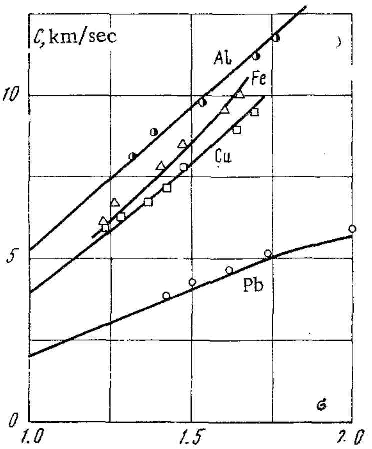

Fig. 4

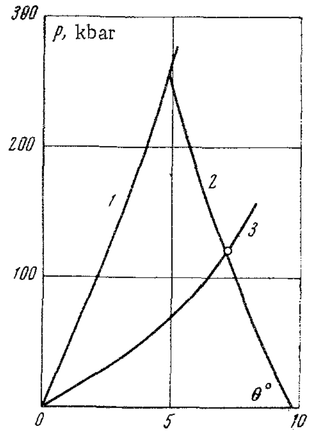

Fig. 5

Fig. 4. Calculated (solid curves) and experimental sound speeds on shock adiabat versus compression ratio for metals.

Fig. 5. 1,3) Shock polars of aluminum and plexiglass for $v_0 = 14.2$ km/sec; 2) unloading polar for aluminum.

$$\frac{dv_r}{d\varphi} = c, \quad v_r = -\frac{1}{\rho c}\frac{dp}{d\varphi}, \quad \rho v_r + c\frac{d\rho}{d\varphi} = 0 \tag{1.2}$$

Excluding $d\varphi$ from the first and third equations (1.2), we obtain

$$v_r dv_r = -c^2 \frac{d\rho}{\rho} \tag{1.3}$$

Integration of (1.3) in the limits of an approximate isentrope segment, on which the speed of sound is constant, yields

$$v_{r,n}^2 - v_{r,n-1}^2 = v_n^2 - v_{n-1}^2 = 2c_{n,n-1}^2 \ln \frac{\rho_{n-1}}{\rho_n} \tag{1.4}$$

Here the subscript n − 1 relates to the upper end of the isentrope segment, and n − 1 applies to the lower end. We obtain the change of the coordinate angle for the given flow region by integrating the first equation (1.2)

$$\varphi_n - \varphi_{n-1} = (v_{r,n} - v_{r,n-1}) / c_{n,n-1} \tag{1.5}$$

The flow deflection angle

$$\theta_{n,n-1} = (\varphi_n + \alpha_n) - (\varphi_{n-1} + \alpha_{n-1}), \qquad \alpha = \operatorname{arc\,tg}\,(c / v_r)) \tag{1.6}$$

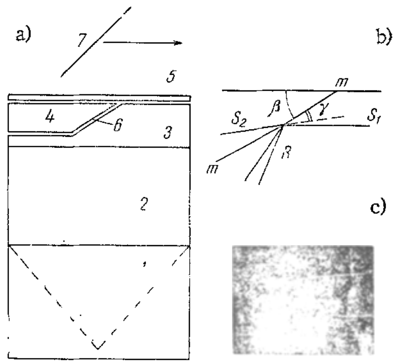

Fig. 6. a) Schematic of experiment to determine refraction parameters: 1) explosive lens; 2) explosive charge; 3) aluminum specimen; 4) Plexiglas specimen, height 10 mm; 5) Plexiglas plate; 6) air gap 0.1 mm thick; 7) mirror, arrow shows ray direction to photorecorder; b) wave configuration; c) typical photochronogram.

where α is the local Mach angle.

If the material isentrope is a broken curve (i.e., the speed of sound changes in jumps) the unloading fan is not continuous. There are flow zones with the same speed of sound, in which unloading takes place; between these zones the pressure, density, and flow velocity v_n are constant (Fig. 3) and correspond to the final values for the preceding rarefaction zone or the initial values for the next zone. The magnitude of the radial velocity component $v_{r,n}^+$ of the flow entering the rarefaction zone is found from the relation

$$v_n^2 = c_{n,n-1}^2 + (v_{r,n}^-)^2 = c_{n,n+1}^2 + (v_{r,n}^+)^2 \tag{1.7}$$

where $v_{r,n}^-$ is the radial component of the flow velocity at the exit from the preceding rarefaction zone.

2. Speed of Sound Calculation. It has been established experimentally that in the coordinates p-u (pressure–mass velocity increment) the unloading isentrope and the two-stage compression shock adiabat for monolithic metals deviate from the single-stage compression shock adiabat by no more than 3% for pressures up to 500 kbar [6]. If we assume that the single-stage and two-stage compression shock adiabats coincide, then as noted in [2] we can write the condition for equality of the pressures in single and double shock compression for the same overall mass velocity increments

$$p(u_1 + u_{1,2}) = p(u_1) + p_{1,2}(u_{1,2}) \tag{2.1}$$

where the subscript 1 denotes the initial parameters ahead of the second shock wave front, and the subscript 1,2 denotes the parameters of the second shock wave. The pressure jump in the shock wave front is $p = \rho_0 Du$. The connection between the shock wave front velocity D and mass velocity jump u is usually represented in the form $D = c_0 + \lambda u$. Therefore Eq. (2.1) may be rewritten as

$$\rho_0 [c_0 + \lambda(u_1 + u_{1,2})](u_1 + u_{1,2}) = \rho_0 (c_0 + \lambda u_1) u_1 + \rho_1 D_{1,2} u_{1,2}$$

Hence we obtain the "second compression" shock adiabat

$$D_{1,2} = c_1 + \lambda_1 u_{1,2}$$

where

$$\lambda_1 = (\rho_0 / \rho_1)\lambda = \lambda / \sigma$$

$$c_1 = \frac{\rho_0}{\rho_1}(c_0 + 2\lambda u_1) = \frac{c_0[\sigma + \lambda(\sigma - 1)]}{\sigma[\sigma - \lambda(\sigma - 1)]} \tag{2.2}$$

It is natural to assume that c_1 is the speed of sound at a given point of the shock adiabat. In fact, comparison of the values calculated using (2.2) with the experimental values presented in [7] from measurement of the speeds of sound in shock-compressed metals shows good agreement (Fig. 4). In calculating the speeds of sound the shock adiabat for aluminum was used in the form $D = 5.25 + 1.39$ u. The shock adiabats of copper, lead, and iron curve markedly with increase of u. For these metals we used the shock adiabats presented in [8], represented in the form of straight line segments with different slopes.

3. Approximate Calculation and Experimental Determination of Oblique Shock Wave Refraction Parameters at Aluminum–Plexiglas Interface. In this study we calculated and verified experimentally for a concrete example the refraction of an oblique shock wave in aluminum at the boundary with Plexiglas.

In the calculation the overall density change in the rarefaction wave is divided into segments of magnitude $\Delta\rho_{n,n-1} = 0.1$ g/cm³. For each segment we used (2.2) to find the mean value of the speed of sound squared $c_{n,n-1}^2$. The corresponding decrease of the pressure on the approximate isentrope was calculated as $\Delta p_{n,n-1} = c_{n,n-1}^2 = \Delta\rho_{n,n-1}$. Here it is assumed that for a fixed density the isentrope slopes are not very sensitive to pressure, which is confirmed by more exact calculations [9]. The remaining flow parameters are found using (1.4)-(1.7). The shock polars for aluminum and Plexiglas and the unloading polar for aluminum calculated for the experimental conditions are shown in Fig. 5. For the calculation of the Plexiglas shock polar we used the shock adiabat in the form D = (2.6 + 1.5 u) km/sec. We see from Fig. 5 that the unloading polar practically coincides with the mirror image of the shock polar. This is apparently due to the small difference between the shock adiabat and the isentrope and the small degree of compression in the shock wave.

The experimental determination of the shock wave front refraction parameters was made using the scheme shown in Fig. 6a. Shock wave front passage through the air gaps was recorded by a high-speed photorecorder operating in the slit scanning mode on the basis of the luminescence of the air. A typical photochronogram is shown in Fig. 6c. The photochronograms were used to determine the shock wave velocity D_0 in the aluminum specimens and the angle γ between the oblique shock wave in the Plexiglas and the interface (Fig. 6b). The latter was calculated from the equation

$$\gamma = \operatorname{arc\,ctg} \frac{D_0\tau / x \sin\beta + \cos\beta}{\sin\beta} \tag{3.1}$$

where β is the angle between the incident shock wave front and the interface; τ and x are the instantaneous coordinates of the oblique shock wave trace in the Plexiglas on the photochronogram. The specimen height in these experiments was 10 mm, the angle $\beta = 30°$. The measured (average of four experiments) parameters were: $D_0 = 7.1 \pm 0.1$ km/sec, $\gamma = 22.36 \pm 0.2°$. The parameters of the oblique shock wave in Plexiglas calculated from γ and $v_0 = D_0/\sin\beta$ have the values: $D_1 = 5.41 \pm 0.05$ km/sec, $p_1 = 119.4 \pm 3$ kbar. We see from Fig. 5 that the agreement between the calculations and experimental values is quite good.

For comparison we can note that for $\beta = 0$ the shock wave velocity in Plexiglas $D_1 = 5.50$ km/sec, which corresponds to p = 126 kbar. From this we can conclude that in the present case, as in the case of oblique shock wave refraction when passing into a medium with higher dynamic stiffness [2], the refraction coefficient $n = D_0/D_1$ changes very little with change of the angle.

4. Refraction Process Stationarity Limit. There is a critical incidence angle β^* upon exceeding which the reflected unloading wave moves away from the interface and the refraction process becomes nonstationary. The angle β^* is determined by equality of the flow velocity behind the shock wave front (relative to the point of intersection of the shock wave front with the interface) and the speed of sound behind the shock wave front, i.e.,

$$(D - u)^2 + D^2 \operatorname{ctg}^2 \beta^* = c^2 \tag{4.1}$$

If the speed of sound is expressed through (2.2) the expression for the magnitude of the critical angle as a function of the shock wave parameters is obtained in the form

$$\operatorname{ctg} \beta^* = (D - u) D^{-2} [\lambda u (2D + \lambda u)]^{1/2} \tag{4.2}$$

Equation (4.2) can be used to calculate the lateral unloading angle when a cylindrical specimen is loaded by a plane shock wave [7].

Knowing the dependence of the critical angle magnitude on the shock wave parameters, we can determine whether or not in the case of condensed media the flow corresponding to the maximal angle of deflection on the shock polar is subsonic relative to the oblique shock wave front. It is shown in [5] that in the case of an ideal gas the maximally deflecting flow is subsonic.

In the variables θ (flow deflection angle) and u (mass velocity jump in the shock wave front) the shock polar for condensed media is represented in the form

$$\theta = \arcsin \frac{c_0 + \lambda u}{v_0} - \operatorname{arc\,tg} \frac{c_0 + (\lambda - 1) u}{\sqrt{v_0^2 - (c_0 + \lambda u)^2}} \tag{4.3}$$

The maximal flow deflection angle is defined by the condition $d\theta/du = 0$. After differentiation and simplification, the condition for the maximal flow deflection angle is obtained in the form

$$v_0^2 - D^2 = \lambda u (D - u) \tag{4.4}$$

For this case the shock wave front incidence angle β_m is defined as

$$\operatorname{ctg} \beta_m = D^{-1} (v_0^2 - D^2)^{1/2} = D^{-1} [\lambda u (D - u)]^{1/2} \tag{4.5}$$

Comparison of β^* and β_m shows that for $\lambda \geq 1.5$, $\beta_m > \beta^*$, while for $\lambda < 1.5$ the ratio β^*/β_m increases with increase of u and exceeds the value 1 if

$$\lambda(2\lambda - 3)\,u^2 + c_0(3\lambda - 2)\,u + c_0^2 = 0$$

This implies that in condensed media the maximally deflecting flow may be either subsonic or supersonic. We can make another remark which is significant for practical applications. The conditions at the interface for refraction of an oblique shock wave require equality of the pressures in the refracted and reflected waves and parallelism of the flows, but equality of the flow velocities is not required. Therefore the flow velocity components parallel to the interface in the refracted and reflected waves may differ, i.e., the interface may be a tangential discontinuity.

LITERATURE CITED

1. L. V. Al'tshuler and A. P. Petrunin, "X-ray studies of the compressibility of light substances with oblique shock wave interaction," Zh. Tekhn. Fiz., 31, No. 6 (1961).
2. P. Laharrague, J. Morvan, and J. Thouvenin, Réfraction d'une onde de choc. Comport. milieux denses hautes pressions dynam., Paris-New York (1968).
3. H. M. Sternberg and D. Piacesi, Interaction of oblique detonation waves with iron, Phys. Fluids, 9, No. 7 (1966), p. 1307.
4. A. K. Oppenheim, J. J. Smolen, and Z. J. Zajac, "Vector polar method for the analysis of wave interactions," Combust. and Flame, 12, No. 1 (1968), p. 63.
5. L. D. Landau and E. M. Lifshits, Continum Mechanics [in Russian], Gostekhizdat, Moscow (1953).
6. M. H. Rice, R. G. McQueen, and J. M. Walsh, "Compression of Solids by Strong Shock Waves," in: Dynamic Studies of Solids at High Pressures [Russian translation], Mir, Moscow (1965), p. 9.
7. L. V. Al'tshuler, S. B. Kormer, M. I. Brazhnik, L. A. Vladimirov, M. P. Speranskaya, and A. I. Funtikov, "Isentropic compressibility of aluminum, copper, and lead at high pressures," Zh. Éksperim. Tekh. Fiz., 38, No. 4 (1960).
8. L. V. Al'tshuler, A. A. Bakanova, and R. F. Trunin, "Shock adiabats and zero isotherms of seven metals at high pressures," Zh. Éksperim. Tekh. Fiz., 42, No. 1 (1962).
9. R. G. McQueen, S. P. Marsh, and J. N. Fritz, "Hugoniot equation of state of twelve rocks," J. Geophys. Res., 72, No. 20 (1967), p. 5036.